Published in final edited form as:
Virology. 2010 February 20; 397(2): 369–378. doi:10.1016/j.virol.2009.11.024.

Induction of Angiogenic Chemokine CCL2 by Human Herpesvirus 8 Chemokine Receptor

Young Bong Choi and **John Nicholas***
Sidney Kimmel Comprehensive Cancer Center, Department of Oncology, Johns Hopkins University School of Medicine, Baltimore, Maryland 21287, U.S.A.

Abstract

Human herpesvirus 8 (HHV-8) is associated with Kaposi's sarcoma (KS), an endothelial cell lesion believed to be initiated and driven primarily by cytokine dysregulation. Among the viral proteins suspected as contributing to viral pathogenesis is the lytically expressed viral G protein-coupled receptor (vGPCR), which can induce various cellular cytokines. CC ligand-2 (CCL2/MCP-1) is a vGPCR-regulated angiogenic chemokine found at elevated levels in KS lesions and induced by HHV-8 infection of endothelial cells. Here we show that vGPCR induces CCL2 in endothelial cells via activation of C/EBPβ and that vGPCR and C/EBPβ are critical components of CCL2 induction by HHV-8 infection of endothelial cultures. To our knowledge, this is the first report of vGPCR-mediated cytokine induction, and its characterization, in the context of virus infection. Our results identify a mechanism by which vGPCR can contribute, in a host cell shutoff-independent manner, to viral pathogenesis.

Keywords

HHV-8; vGPCR; ORF74; CCL2; MCP-1; angiogenesis; C/EBPβ; transcription

Introduction

Human herpesvirus 8 (HHV-8) has been linked to Kaposi's sarcoma (KS) in addition to certain B cell lymphomas (Ablashi et al., 2002; Chang et al., 1994; Hengge et al., 2002). There is substantial evidence that the development of KS is in large part driven by angiogenic and pro-inflammatory cytokine dysregulation, and the contribution of HHV-8 to the onset and progression of disease is generally thought to involve induction of such cytokines to promote endothelial cell proliferation and angiogenesis characteristic of KS (Ensoli, Sturzl, and Monini, 2001; Jensen and Lira, 2004). Several HHV-8 encoded proteins have been implicated in this process. The signal transducing membrane proteins specified by ORFs K1 and K15 have been reported to induce KS-associated cytokines such as VEGF, IL-6 and CXCL8 (Brinkmann et al., 2007; Lee et al., 2005; Prakash et al., 2005; Samaniego et al., 2001; Wang et al., 2004), viral interleukin-6 can induce expression of VEGF and CCL2, for example (Aoki et al., 1999; Fielding et al., 2005), and multiple angiogenic cytokines, including VEGF, CCL2, CXCL1, CXCL8, IL-1β, bFGF, and angiopoietin-2, are

*Corresponding author. Phone: 410 502 6801; Fax: 410 502 6802; nichojo@jhmi.edu.

induced by the viral G protein-coupled receptor (vGPCR) specified by ORF74 (Bais et al., 1998; Martin et al., 2008; Pati et al., 2001; Schwarz and Murphy, 2001; Vart et al., 2007). Such cytokines could contribute to the onset and progression of KS. When introduced into mice, vGPCR is able to induce lesions that resemble KS (Montaner et al., 2003; Yang et al., 2000). Importantly, this is possible with expression of vGPCR in only a small minority of cells in the tumor, implicating receptor-induced cytokines (i.e., paracrine signaling) in this process. Indeed, all available evidence indicates that vGPCR is expressed exclusively during lytic replication, rather than latency (Chiou et al., 2002; Jeong, Papin, and Dittmer, 2001; Kirshner et al., 1999; Nador et al., 2001), suggesting that only paracrine contributions of vGPCR to KS are possible. However, only those cytokines that can escape virus-induced host cell shutoff (destabilization of cellular mRNAs) are potentially available to contribute to viral pathogenesis in this way (Glaunsinger and Ganem, 2004a; Glaunsinger and Ganem, 2004b). CCL2, the focus of this manuscript, is one such cytokine that can both escape host-cell shutoff and potentially contribute via its pro-angiogenic activity to KS.

While many studies of vGPCR activity in respect of signal transduction, induced cellular genes, and effects on cell growth *in vitro* and *in vivo* have been reported using vGPCR-transduced cells, investigations of vGPCR activity in the context of HHV-8 infection are lacking. In view of this and the potential of vGPCR to contribute to KS pathogenesis via cytokine induction, within the restrictions imposed by widespread host cell shutoff, we wanted to investigate the mechanisms of vGPCR-mediated angio-cytokine induction in the context of virus infection as well as in isolation. Our data identify CCL2 as a cytokine induced robustly by vGPCR in endothelial cells, determine that MAPK-activated C/EBPβ is necessary for the induction, and demonstrate the relevance of vGPCR and C/EBPβ for CCL2 induction during HHV-8 infection of endothelial cells.

Results and Discussion

To provide a means of analyzing vGPCR function in endothelial cells, we used commercially available retroviral vectors (*Tet-On Advanced*, Clontech) to generate telomerase immortalized endothelial (TIME) cells (Venetsanakos et al., 2002) in which vGPCR expression was inducible by doxycycline (Dox) treatment. These TIME-vGPCR cells showed appropriate Dox-inducible expression of vGPCR, as determined by immunofluorescence assay and western blotting (Fig.1A), in addition to qRT-PCR analysis (>500-fold induction, data not shown). A focused gene array representing angiogenic cytokines and regulators (see Materials and Methods) was used to identify vGPCR-regulated genes via hybridization of cRNA probes derived from Dox-treated versus untreated TIME-vGPCR cells. While vGPCR affected expression of several genes (data not shown), CCL2 showed particularly strong induction (Fig.1B). The array data were confirmed by qRT-PCR analysis of RNA extracted from TIME-vGPCR cells maintained in the absence and presence of Dox; there was a marked induction (>6-fold) of CCL2 mRNA expression in response to Dox (Fig.1C, top). Similarly, Dox treatment was able to induce expression of secreted CCL2, detected and quantified using ELISA assay (Fig.1C, bottom). CCL2 was produced in biologically significant amounts, the concentration in culture media achieved during the 24 h induction period reaching 9 ng/ml (approximating the ED50 for chemoattraction). Our data were consistent with previous reports of robust induction of CCL2 mRNA and protein by vGPCR (Martin et al., 2008; Schwarz and Murphy, 2001). As CCL2 has been demonstrated to be expressed in KS lesions, to be induced by HHV-8 infection of endothelial cells (and therefore not subject to host cell shutoff), and to signal in endothelial cells to promote angiogenesis (Caselli et al., 2007; Salcedo et al., 2000; Sciacca et al., 1994; Stamatovic et al., 2006; Uccini et al., 2003), we sought characterize the mechanism of vGPCR-mediated CCL2 induction.

RNA polymerase II (PolII)-based chromatin immunoprecipitation (ChIP) experiments were undertaken to verify that the effects seen were due to transcriptional induction by vGPCR. Primers for amplification of immunoprecipitated DNA were directed to promoter and 3' regions of the CCL2 gene (Fig.2A). CCL2 promoter-associated PolII was enhanced by Dox-induced vGPCR expression (Fig.2B), thereby confirming transcriptional regulation of CCL2 by the viral receptor. Around 3-fold induction of CCL2 promoter-associated PolII in response to vGPCR expression was evident from qPCR analysis of precipitated DNA (Fig. 2C, left). A similar result was obtained by analogous comparison of uninfected and HHV-8 *de novo* infected TIME cells (Fig.2C, right), indicating transcriptional induction of CCL2 by infection also.

CCL2 promoter, enhancer and 3' regions, containing demonstrated or predicted transcription factor binding sites (Fig.2A), had previously been implicated in transcriptional regulation of CCL2 (Abraham et al., 2005;Mukerjee et al., 2008;Tanimoto et al., 2008;Ueda et al., 1994;Wolter et al., 2008). Using appropriate antibodies for ChIP and PCR primer pairs to these regulatory regions (Fig.2A), the potential involvement of NF-κB, Jun, ATF2, Ets-1 and C/EBPβ in regulation of the chemokine gene by vGPCR was investigated. This series of ChIP assays identified vGPCR-induced association of C/EBPβ, specifically, with regions of the CCL2 gene corresponding to 5' promoter and 3' distal sequences, amplified by PCR primer pairs 4 and 6 (Fig.2D). Putative C/EBPβ binding sites lie immediately adjacent or close to the PCR-amplified products (well within 300bp, the approximate upper size limit of sonicated, immunoprecipitated DNA). These data indicated the likely involvement of C/EBPβ in CCL2 induction by vGPCR, and the potential relevance of promoter-proximal and 3' *cis*-elements in this activity. To test the latter, these sequences were cloned into a luciferase reporter plasmid, in their appropriate 5' and 3' positions, and transfected into HEK293T cells. The 5' region (-560/+1), alone, was responsive to vGPCR expression (Fig. 3A). To better define responsive sequences within the 5' region, deletion mutagenesis was undertaken, and single or combined mutagenesis of the putative C/EBPβ binding sites was carried out to test directly the relevance of these elements. The respective reporter constructions were used in transfection experiments, as before. The results revealed that deletion of sequences between -320 and -240, containing the proximal C/EBP consensus site, led to loss of vGPCR responsiveness, and that specific mutation of the proximal C/EBP *cis*-element, but not the more distal site, was alone sufficient to abrogate vGPCR-mediated induction (Fig.3B). These data, taken together with the ChIP analysis, indicated the significance C/EBPβ and the proximal C/EBP site at -256 to -263 for transcriptional induction of CCL2 by vGPCR.

To verify the targeting and activation of C/EBPβ by vGPCR, EMSA and immunoblotting approaches were employed. For EMSA, a wild-type C/EBP probe or a C/EBP site-mutated version (see Materials and Methods) were mixed with nuclear extracts derived from parallel cultures of TIME-vGPCR cells either treated with Dox ($vGPCR^+$) or left untreated, prior to PAGE analysis. Formation of C/EBP binding site dependent DNA-protein complexes was increased as a function of vGPCR expression (Fig.4A). These complexes could be competed with an excess of unlabeled wild-type but not C/EBP core sequence-mutated probe (lanes 4-7), confirming interaction specificity. That C/EBPβ comprised a major component of the detected complexes was evidenced by their supershifting with addition of C/EBPβ antibody (Fig.4A, lanes 8 and 9). Antibody to NF-κB component p65, used as a negative control, did not affect migration of the complexes (Fig.4A, lanes 10 and 11). Together, the EMSA data indicated that C/EBPβ was a target of activation by vGPCR signaling. This was verified by immunoblotting for phosphorylated (activated) C/EBPβ at various times after Dox application to TIME-vGPCR cultures. The phospho-specific antibody used for western blotting was directed to threonine-235, a known target of the mitogen activated protein kinase (MAPK) ERK and phosphorylation of which leads to activation of C/EBPβ DNA

binding and transcriptional activity (Hu et al., 2001;Hungness et al., 2002). Phosphorylation of C/EBPβ was induced rapidly (within 3 h) by Dox treatment, with levels of total C/EBPβ unchanged (Fig.4B, top two panels). Consistent with these findings, concomitant phosphorylation (activation) of C/EBPβ-activating ERK was detected in response to Dox-induced vGPCR expression (Fig.4B, middle two panels). Kinetics of Dox-induced vGPCR expression, as determined by western blotting (Fig.4B, bottom two panels), matched the activation profiles of C/EBPβ and ERK. Thus, our EMSA and immunoblotting data demonstrate that vGPCR can induce activation of C/EBPβ in endothelial cells, consistent with the ChIP data implicating C/EBPβ as a potential effector of CCL2 induction by vGPCR (Fig.2).

To address directly the relevance of C/EBPβ for vGPCR-mediated CCL2 induction, TIME cells expressing either of two active C/EBPβ-directed shRNAs (Fig.5A) or non-silencing (NS) shRNA control were transduced with vGPCR-expressing or empty lentiviral vectors. Following incubation for 24 h, mRNA was extracted for qRT-PCR analysis of CCL2 transcript levels. vGPCR-induced CCL2 mRNA expression was diminished strongly by C/EBPβ depletion by each of the C/EBPβ shRNAs, but not by the NS control shRNA, confirming the importance of C/EBPβ for vGPCR-induced CCL2 expression (Fig.5B). A similar experiment was undertaken in the absence and presence of MEK (ERK kinase) inhibitor PD98059, demonstrating the importance for vGPCR-mediated CCL2 induction of MAPK pathway activation, consistent with C/EBPβ activation being mediated via this route (Fig.5C). In contrast, PD98059 had no effect on TNFα-mediated CCL2 activation, demonstrating the specificity of action of the MEK inhibitor.

Finally, experiments were undertaken to assess the relevance of vGPCR and C/EBPβ to CCL2 induction in the context of HHV-8 infection. *De novo* infection of TIME cells with BCBL-1 derived HHV-8 [as described previously (Choi and Nicholas, 2008)] and qRT-PCR analysis of CCL2 mRNA expression at different times (0 to 3 days) post-infection verified the induction of CCL2 by HHV-8 (Fig.6A), previously reported in human umbilical vein endothelial cells (Caselli et al., 2007). The involvement of vGPCR in this process was addressed by its depletion, using two pre-validated shRNAs (Fig.6B). These were transduced into TIME cells using lentiviral vectors [to achieve an infection rate (GFP^+) of >90%], and cultures subsequently infected with HHV-8. Each of the vGPCR-directed shRNAs led to dramatic reductions, relative to control NS shRNA, of qRT-PCR-detected CCL2 induction by HHV-8 infection (Fig.6C, top). Measurements of secreted CCL2 protein levels in NS and vGPCR-sh2 shRNA-transduced cultures after 2 and 3 days of Dox treatment (Fig.6C, bottom) reflected the qRT-PCR results. These data provide strong evidence of the involvement of and requirement for vGPCR in HHV-8-induced CCL2 expression. The depletion approach was also used to address the relevance of C/EBPβ for CCL2 induction by HHV-8 infection. Cells expressing either of our two C/EBPβ shRNAs (Fig.5A) showed diminished CCL2 induction in response to HHV-8 *de novo* infection, thereby confirming the involvement of C/EBPβ in this process (Fig.6D). The relevance of vGPCR in activation of C/EBPβ in the context of HHV-8 infection was verified by immunoblotting for phosphorylated (activated) C/EBPβ in the absence and presence of vGPCR depletion in cells infected *de novo* with HHV-8; C/EBPβ activation was reduced significantly in vGPCR shRNA-transduced cells (Fig.6E). Appropriate infection of TIME cells and expression of vGPCR was checked by infection of cultures under identical conditions and detection by immunofluorescence staining of vGPCR. Co-staining for latency-associated nuclear antigen (LANA), expression of which occurs within hours after *de novo* infection and persists during subsequent latent infection of inoculated cells (Sadagopan et al., 2007; Sharma-Walia et al., 2005), was undertaken to identify infected cells. High infection rates ($LANA^+$ cells) were detected, and most of these cells also expressed detectable levels of vGPCR at 24 h post-infection (Fig.6F). These data

demonstrate the rapid and widespread expression of vGPCR in endothelial cells following *de novo* infection.

The mechanism by which vGPCR might contribute to KS pathogenesis is unclear, but present evidence favors a paracrine function of vGPCR in viral pathogenesis, because vGPCR expression has been detected only during lytic replication. Data presented here as well as previously (Caselli et al., 2007) indicate that CCL2 is a host cytokine that can escape virus-induced host shutoff (Glaunsinger and Ganem, 2004a; Glaunsinger and Ganem, 2004b) and potentially contribute to KS via its angiogenic activity. While it has been reported that HHV-8 infection of endothelial cells activates NF-κB and that this is important for virus-mediated CCL2 induction, the reporter-luciferase experiments presented in this previous study in fact showed that mutation of NF-κB *cis*-elements affected overall CCL2 promoter activity rather than fold-induction by HHV-8 infection (Caselli et al., 2007). Indeed, this study reported that other NF-κB-inducible cytokines, such as CXCL8/IL-8 and CCL5/RANTES, were not induced by HHV-8 infection. In agreement with this previous study, we found that CCL2 was the major angiogenic/pro-inflammatory cytokine induced by HHV-8 infection. However, our analysis of endogenous CCL2 promoter-associated transcription factor activation by ChIP assays identified C/EBPβ activation as of likely primary relevance, rather than NF-κB activation. This was verified by C/EBPβ depletion experiments showing marked diminution of HHV-8 mediated CCL2 induction in the presence of C/EBPβ-directed shRNAs. Furthermore, vGPCR depletion led to almost complete loss of CCL2 induction in response to HHV-8 infection. Thus, while other viral signaling proteins, such as vIL-6 and K15 encoded membrane protein, shown to induce CCL2 in experimental systems (Brinkmann et al., 2007; Fielding et al., 2005), can potentially contribute to this process, our data implicate vGPCR as critically important. Data from our ChIP and reporter assays indicate that C/EBPβ binding to the CCL2 promoter is induced by vGPCR, that at least one vGPCR-responsive element of the CCL2 promoter lies within the -560/+1 region, and that the putative C/EBP binding site at -256 to -263 is functionally significant. We have not ruled out the possibility that other functionally relevant C/EBPβ-binding *cis*-elements may lie outside this region, however. Further studies will be required to determine whether other promoter and/or enhancer elements are involved in responsiveness of the CCL2 promoter to vGPCR signaling and HHV-8 infection, and to elucidate possible co-contributions of other HHV-8 signaling proteins. Notwithstanding, the data presented here identify vGPCR as essential for activation of CCL2 expression by HHV-8 *de novo* infection of endothelial cells and establish that this activity is mediated primarily by C/EBPβ activation via MAPK pathway signaling.

Materials and Methods

Plasmids and oligonucleotides

HHV-8 open reading frame 74 (ORF74, encoding vGPCR) was cloned between the *Bam*HI and *Mlu*I sites of pRetroX-Tight-Pur (Clontech Laboratories Inc., Mountain View, CA). Human genomic DNA fragments encompassing CCL2 promoter (-560 to +60), truncated versions thereof, or 3’ region of the CCL2 gene (UTR+3’-region, +1539 to +2558) were amplified and cloned between the *Mlu*I and *Xho*I sites or into the *Xba*I site, respectively, of pGL3 basic (Promega, Madison, WI). Complementary pairs of 59-nucleotide oligonucleotides encoding a 21-nucleotide short hairpin RNA (shRNA) to C/EBPβ (sh1: 5’-cccgtggtgttatttaaagaa-3’ and sh2: 5’-tgtgtacagatgaatgataaa-3’) and vGPCR (sh1: 5’-agcggatatgactactctgga-3’ and sh2: 5’-aacgttggaatactctctctg-3’) mRNA sequences, or non-silencing (NS) control (Choi and Nicholas, 2008), were annealed and cloned between the *Bam*HI and *Mlu*I sites of lentiviral vector pYNC352 (Choi and Nicholas, 2008). Primer sequences used for quantitative PCR were the following: CCL2 forward primer (5’-aagatctcagtgcagaggctcg-3’); CCL2 reverse primer (5’-ttgcttgtccaggtggtccat-3’); vGPCR

forward primer (5'-gtggtgccttacacgtggaa-'3); vGPCR reverse primer (5'-gcgagtttaggcagatacccag-3'); 18S forward primer (5'-cgcggttctattttgttggt-3'); 18S reverse primer (5'-ccctcttaatcatggcctca-3'). Primer sequences used for ChIP were the following: forward primer-1 (5'-ctggaatgcaggctccagcca-3'); reverse primer-1 (5'-cctttgcatatatcagacagt-3'); forward primer-2 (5'-ccttgagcaggctatttaacc-3'); reverse primer-2 (5'-cttggacaaaggcatagacag-3'); forward primer-3 (5'-ttaatgcattgtcagggagcc-3'); reverse primer-3 (5'-ggaagcgaggaaactagatga-3'); forward primer-4 (5'-tggcaccccatcctccccatt-3'); reverse primer-4 (5'-ctctcggttcctctggctgct-3'); forward primer-5 (5'-gtaaggccccctcttcttctc-3'); reverse primer-5 (5'-ccagagctggaatcctggaag-3'); forward primer-6 (5'-ccagatgcgaattcgggccca-3'); reverse primer-6 (5'-tggaccatggcaatagcttct-3'). PCR products using primer pairs 1-5 correspond to CCL2 promoter/enhancer sequences -2459 to -2639, -766 to -560, -454 to -327, -240 to -1, and +33 to +369, respectively, and primer pair 6 amplifies the +2550 to +2807 region 3' of the mRNA coding sequences. Progressively 5'-deleted segments of the CCL2 promoter region were obtained by PCR using the following primers in concert with +60-reverse primer (5'-ggctggaggcgagagtgcgagc-3'): -560-forward (5'-gtctgaaaccctagaactctt-3'); -480-forward (5'-ttctgcatttgaatgagcaaa-3'); -400-forward (5'-ggccccttggaatgtggcctg-3'); -320-forward (5'-tctgcagttttcgcttcagag-3'); -240-forward (5'-tggcaccccatcctccccatt-3'); -160-forward (5'-tttcctacttcctggaaatcc -3'); -80-forward (5'-ctcctcctgcttgactccgcc-3'). Mutagenesis of putative C/EBP sites within the promoter region was carried out using Pfx DNA polymerase in PCR-based procedures to replace C/EBP sites (positions -516 to -523 and -256 to -263) with an *Spe*I site-containing sequence (cACTAGTc), used for subsequent identification of luciferase reporter-cloned mutated promoter sequences. Primers used for mutagenic PCR were: -520F-C/EBP-mut (5'-cttagaattcagttcaatgtCACTaGTCtcctacagttctgctaggct-3'; upper case, mutated nucleotides); -520R-C/EBP-mut (reverse complement of -520-C/EBP-mut); -260F-C/EBP-mut (5'-aataaccctcttagttcacaCACTAgTCcagtctgggcttaatggcac-3'); -260R-C/EBP-mut (reverse complement of -260F-C/EBP-mut). Primer sequences used for EMSA were the following: C/EBPβ (5'-tgcagattgcgcaatctgca-3') and mutated C/EBPβ (5'-tgcagagactagtctctgca-3'), together with the respective complements.

Antibodies

RNA polymerase II (N-20), NF-κB p65 (A), C/EBPβ (C-19), Ets-1 (C-20), c-Jun (D), and ATF-2 (N-96) antibodies were purchased from Santa Cruz Biotechnology, Inc. (Santa Cruz, CA); phospho-C/EBPβ (Thr235), phospho-Erk1/2 (Thr202/Tyr204), and Erk1/2 antibodies were purchased from Cell Signaling Technology, Inc. (Beverly, MA); β-actin antibody was purchased from Sigma (St. Louis, MO); CCR8 and GFP antibodies were from Epitomics, Inc. (Burlingame, CA). ELISA for CCL2/MCP-1 was undertaken using reagents and procedures from Peprotech (Rocky Hill, NJ) to determine CCL2 protein concentrations in culture media. Previously described rabbit antiserum directed to the N-terminal region of vGPCR (Chiou et al., 2002) was kindly provided by Dr. Gary Hayward.

Cell culture, transfection, transduction, and infection

Telomerase immortalized microvascular endothelial (TIME) cells (Venetsanakos et al., 2002) were maintained in EGM-2 MV medium (Lonza, Walkersville, MD) containing 5% fetal bovine serum (FBS) and cytokine supplements. HEK293T cells were grown in Dulbecco's modified Eagle's medium supplemented with 10% FBS and gentamicin. BCBL-1 cells were cultured in RPMI 1640 supplemented with 20% heat-inactivated FBS and gentamicin. For virus vector production or reporter assays, HEK293T cells were transiently transfected with plasmid DNA using standard calcium phosphate co-precipitation. Stable transduction of TIME cells with retrovirus (for shRNA expression) or lentivirus (for protein expression) was performed under puromycin selection. Infectious HHV-8 virus was obtained by inducing BCBL-1 cells with phorbol 12-myristate 13-acetate (PMA; 20 ng/ml)

and calcium ionophore (A23187; 500 ng/ml). After 20 h, cells were pelleted and resuspended in fresh medium without PMA and A23187. After four days, virions were pelleted from culture media by centrifugation at 15,000 rpm for 2 h in an SW41 rotor. For HHV-8 infection of TIME cells, the viral pellet was resuspended in basal EGM-2 MV medium supplemented with Polybrene (5 μg/ml) and added to cell cultures for 2 h, prior to replacement of inoculum with fresh medium. In experiments to determine the influence of virus-produced vGPCR on C/EBPβ phosphorylation, culture medium containing 1% serum and no cytokine supplements was employed to minimize background (non-virus-induced) C/EBPβ activation.

Membrane array expression analysis

Total RNA from TIME-vGPCR cells treated with 1 μg/ml doxycycline or mock treated (carrier, DMSO, only) for 24 h were isolated with the RNeasy RNA purification kit (Qiagen, Valencia, CA). RNA was reverse transcribed using the TrueLabeling-AMP™ 2.0 kit (Superarray, Frederick, MD), to obtain cDNA and converted into biotin-labeled cRNA using biotin-16-UTP (Roche Applied Science, Indianapolis, IN) by *in vitro* transcription. cRNA probes were purified with the ArrayGrade cRNA cleanup kit (Superarray) and then hybridized to the pretreated Oligo GEArray® Human Angiogenesis Microarray OHS-024 (Superarray). Following several washing steps, array spots binding cRNA were detected using alkaline phosphatase-conjugated streptavidin and CDP-Star as chemiluminescent substrate and visualized on X-ray film.

Quantitative RT-PCR

First-strand cDNA was synthesized from 1 μg of total RNA using SuperScript II reverse transcriptase (Invitrogen, Carlsbad, CA) with random hexamers. SYBR green-based quantitative PCR was performed using the 7500 real-time PCR system (Applied Biosystems, Carlsbad, CA). PCR conditions included an initial incubation step of 2 min at 50°C and an enzyme heat activation step of 10 min at 95°C, followed by 50 cycles of 15 seconds at 95°C for denaturing and 1 min at 60°C for annealing and extension.

Immunoblotting and Immunofluorescence assay

For general immunoblotting, cells were lysed in lysis buffer (50 mM Tris-HCl [pH 8.0], 150 mM NaCl, 1 mM EDTA, 1% IGEPAL CA-630, 0.25% sodium deoxycholate, and protease and protein phosphatase inhibitor cocktails). For extraction of integral membrane proteins vGPCR and CCR8, cell pellets were suspended in 0.25M sucrose supplemented with protease inhibitors and cells disrupted by sonication; nuclei were removed by centrifugation at 1,000g for 10 min. and membranes pelleted by centrifugation at 20,000g for 1 h, prior to protein solubilization in CHAPS buffer (100 mM Tris-HCl, [pH 7.4], 50 mM NaCl, 5 mM EDTA, and 1% CHAPS) overnight at 4°C. Cell extract- or membrane-derived proteins were size fractionated by sodium dodecyl sulfate-polyacrylamide gel electrophoresis (SDS-PAGE) and transferred to a nitrocellulose membrane. Immunoreactive bands were detected with enhanced chemiluminescence solution (GE Healthcare, Piscataway, NJ) and visualized on X-ray film. For immunofluorescence assay (IFA), cells on a 0.1% gelatin-coated coverglass were fixed and permeabilized in chilled methanol. Following incubation with blocking buffer (3% bovine serum albumin in PBS), coverslips were incubated with primary antibody, washed with phosphate-buffered saline (PBS), and then incubated with appropriate fluorescent dye-conjugated secondary antibody. Coverslips were mounted in 90% glycerol in PBS containing 10 mg/ml *p*-phenylenediamine. Nuclei were visualized by staining with Hoechst 33342.

Chromatin Immunoprecipitation (ChIP) assay

ChIP assay was performed according to the protocol of Nelson et al. (Nelson, Denisenko, and Bomsztyk, 2006). Briefly, cells were fixed with formaldehyde in a final concentration of 1.42% for 10 min at room temperature and then incubated with 125 mM glycine for 5 min at room temperature to quench the formaldehyde. The cells were washed with ice-cold PBS twice and lysed in 1 ml of immunoprecipitatin (IP) buffer (150 mM NaCl, 50 mM Tris-HCl [pH 7.5], 5 mM EDTA, 0.5% IGEPAL CA-630, 1% Triton X-100, and protease inhibitor cocktail). The lysates were centrifuged at 12,000g for 1 min at 4°C. The nuclear pellet was washed with IP buffer, resuspended in 400 μl of IP buffer, and then sonicated ten times by 20-second pulses on ice under the 30% amplitude setting of Branson sonicator 185 (Danbury, CT). The lysate was cleared by centrifugation at 12,000g for 10 min at 4°C and incubated with the antibody for 12 h. The immune complex was precipitated with protein A-agarose and then washed six times with 1 ml cold IP buffer. DNA fragments in the complex were released by boiling for 5 min with 10% Chelex 100 slurry. The supernatant was treated with proteinase K (200 ng/ml) at 55°C for 30 min and then boiled for 10 min. DNA fragments were purified with phenol/chloroform, concentrated by ethanol precipitation with 20 μg of glycogen, and subjected to quantitative PCR. DNA copy number was determined from a standard curve generated by each primer set with known amounts of genomic DNA.

Reporter assay

HEK293T cells were transiently transfected with pSG5 or pSG5-vGPCR plasmids along with reporter plasmids for 24 h and then lysed with passive lysis buffer (Promega, Madison, WI). Luciferase activity was measured by standard protocol using D-luciferin.

Electrophoretic mobility shift assay

Nuclear extracts from doxycycline-treated or untreated TIME-vGPCR cells were prepared by homogenization using buffer A (10 mM HEPES [pH 8.0], 1.5 mM $MgCl_2$, 10 mM KCl, 0.5 mM DTT, and protease inhibitor) and after centrifugation resuspending pellet in buffer B (20 mM HEPES [pH 8.0], 1.5 mM $MgCl_2$, 420 mM NaCl, and 0.2 mM EDTA). The nuclear extracts (10 μg protein) were incubated in the presence of 2 ng of radiolabeled oligonucleotides in binding buffer (10 mM Tris-HCl, pH 8.0, 150 mM KCl, 0.2 mM DTT, 0.5 mM EDTA, 12.5% glycerol, and 1 μg of poly(dI-dC)). For supershift assay, the nuclear extracts were incubated with 200 ng of appropriate antibodies for 30 min at room temperature and then for 15 min with the oligonucleotide. For competition assay, 20 ng of unlabeled oligonucleotide was added to the reaction mixture. Complexes were electrophoresed on 4% acrylamide gel, dried, and visualized by autoradiography.

Acknowledgments

The work presented in this manuscript was supported by grants R21-CA119887 and P01-CA113239 from the National Cancer Institute.

References

Ablashi DV, Chatlynne LG, Whitman JE Jr. Cesarman E. Spectrum of Kaposi's sarcoma-associated herpesvirus, or human herpesvirus 8, diseases. Clin Microbiol Rev 2002;15(3):439–64. [PubMed: 12097251]

Abraham S, Sweet T, Sawaya BE, Rappaport J, Khalili K, Amini S. Cooperative interaction of C/EBP beta and Tat modulates MCP-1 gene transcription in astrocytes. J Neuroimmunol 2005;160(1-2): 219–27. [PubMed: 15710476]

Aoki Y, Jaffe ES, Chang Y, Jones K, Teruya-Feldstein J, Moore PS, Tosato G. Angiogenesis and hematopoiesis induced by Kaposi's sarcoma-associated herpesvirus-encoded interleukin-6. Blood 1999;93(12):4034–43. [PubMed: 10361100]

Bais C, Santomasso B, Coso O, Arvanitakis L, Raaka EG, Gutkind JS, Asch AS, Cesarman E, Gershengorn MC, Mesri EA. G-protein-coupled receptor of Kaposi's sarcoma-associated herpesvirus is a viral oncogene and angiogenesis activator. Nature 1998;391(6662):86–9. [PubMed: 9422510]

Brinkmann MM, Pietrek M, Dittrich-Breiholz O, Kracht M, Schulz TF. Modulation of host gene expression by the K15 protein of Kaposi's sarcoma-associated herpesvirus. J Virol 2007;81(1):42–58. [PubMed: 17050609]

Caselli E, Fiorentini S, Amici C, Di Luca D, Caruso A, Santoro MG. Human herpesvirus 8 acute infection of endothelial cells induces monocyte chemoattractant protein 1-dependent capillary-like structure formation: role of the IKK/NF-kappaB pathway. Blood 2007;109(7):2718–26. [PubMed: 17138827]

Chang Y, Cesarman E, Pessin MS, Lee F, Culpepper J, Knowles DM, Moore PS. Identification of herpesvirus-like DNA sequences in AIDS-associated Kaposi's sarcoma. Science 1994;266(5192): 1865–9. [PubMed: 7997879]

Chiou CJ, Poole LJ, Kim PS, Ciufo DM, Cannon JS, ap Rhys CM, Alcendor DJ, Zong JC, Ambinder RF, Hayward GS. Patterns of gene expression and a transactivation function exhibited by the vGCR (ORF74) chemokine receptor protein of Kaposi's sarcoma-associated herpesvirus. J Virol 2002;76(7):3421–39. [PubMed: 11884567]

Choi YB, Nicholas J. Autocrine and paracrine promotion of cell survival and virus replication by human herpesvirus 8 chemokines. J Virol 2008;82(13):6501–13. [PubMed: 18434408]

Ensoli B, Sturzl M, Monini P. Reactivation and role of HHV-8 in Kaposi's sarcoma initiation. Adv Cancer Res 2001;81:161–200. [PubMed: 11430595]

Fielding CA, McLoughlin RM, Colmont CS, Kovaleva M, Harris DA, Rose-John S, Topley N, Jones SA. Viral IL-6 blocks neutrophil infiltration during acute inflammation. J Immunol 2005;175(6): 4024–9. [PubMed: 16148151]

Glaunsinger B, Ganem D. Highly selective escape from KSHV-mediated host mRNA shutoff and its implications for viral pathogenesis. J Exp Med 2004a;200(3):391–8. [PubMed: 15289507]

Glaunsinger B, Ganem D. Lytic KSHV infection inhibits host gene expression by accelerating global mRNA turnover. Mol Cell 2004b;13(5):713–23. [PubMed: 15023341]

Hengge UR, Ruzicka T, Tyring SK, Stuschke M, Roggendorf M, Schwartz RA, Seeber S. Update on Kaposi's sarcoma and other HHV8 associated diseases. Part 2: pathogenesis, Castleman's disease, and pleural effusion lymphoma. Lancet Infect Dis 2002;2(6):344–52. [PubMed: 12144897]

Hu J, Roy SK, Shapiro PS, Rodig SR, Reddy SP, Platanias LC, Schreiber RD, Kalvakolanu DV. ERK1 and ERK2 activate CCAAAT/enhancer-binding protein-beta-dependent gene transcription in response to interferon-gamma. J Biol Chem 2001;276(1):287–97. [PubMed: 10995751]

Hungness ES, Pritts TA, Luo GJ, Hershko DD, Robb BW, Hasselgren PO. IL-1beta activates C/EBP-beta and delta in human enterocytes through a mitogen-activated protein kinase signaling pathway. Int J Biochem Cell Biol 2002;34(4):382–95. [PubMed: 11854037]

Jensen KK, Lira SA. Chemokines and Kaposi's sarcoma. Semin Cancer Biol 2004;14(3):187–94. [PubMed: 15246054]

Jeong J, Papin J, Dittmer D. Differential regulation of the overlapping Kaposi's sarcoma-associated herpesvirus vGCR (orf74) and LANA (orf73) promoters. J Virol 2001;75(4):1798–807. [PubMed: 11160678]

Kirshner JR, Staskus K, Haase A, Lagunoff M, Ganem D. Expression of the open reading frame 74 (G-protein-coupled receptor) gene of Kaposi's sarcoma (KS)-associated herpesvirus: implications for KS pathogenesis. J Virol 1999;73(7):6006–14. [PubMed: 10364352]

Lee BS, Lee SH, Feng P, Chang H, Cho NH, Jung JU. Characterization of the Kaposi's sarcoma-associated herpesvirus K1 signalosome. J Virol 2005;79(19):12173–84. [PubMed: 16160144]

Martin D, Galisteo R, Ji Y, Montaner S, Gutkind JS. An NF-kappaB gene expression signature contributes to Kaposi's sarcoma virus vGPCR-induced direct and paracrine neoplasia. Oncogene 2008;27(13):1844–52. [PubMed: 17934524]

Montaner S, Sodhi A, Molinolo A, Bugge TH, Sawai ET, He Y, Li Y, Ray PE, Gutkind JS. Endothelial infection with KSHV genes in vivo reveals that vGPCR initiates Kaposi's

sarcomagenesis and can promote the tumorigenic potential of viral latent genes. Cancer Cell 2003;3(1):23–36. [PubMed: 12559173]

Mukerjee R, Deshmane SL, Darbinian N, Czernik M, Khalili K, Amini S, Sawaya BE. St. John's Wort protein, p27SJ, regulates the MCP-1 promoter. Mol Immunol 2008;45(15):4028–35. [PubMed: 18649942]

Nador RG, Milligan LL, Flore O, Wang X, Arvanitakis L, Knowles DM, Cesarman E. Expression of Kaposi's sarcoma-associated herpesvirus G protein-coupled receptor monocistronic and bicistronic transcripts in primary effusion lymphomas. Virology 2001;287(1):62–70. [PubMed: 11504542]

Nelson JD, Denisenko O, Bomsztyk K. Protocol for the fast chromatin immunoprecipitation (ChIP) method. Nat Protoc 2006;1(1):179–85. [PubMed: 17406230]

Pati S, Cavrois M, Guo HG, Foulke JS Jr. Kim J, Feldman RA, Reitz M. Activation of NF-kappaB by the human herpesvirus 8 chemokine receptor ORF74: evidence for a paracrine model of Kaposi's sarcoma pathogenesis. J Virol 2001;75(18):8660–73. [PubMed: 11507211]

Prakash O, Swamy OR, Peng X, Tang ZY, Li L, Larson JE, Cohen JC, Gill J, Farr G, Wang S, Samaniego F. Activation of Src kinase Lyn by the Kaposi sarcoma-associated herpesvirus K1 protein: implications for lymphomagenesis. Blood 2005;105(10):3987–94. [PubMed: 15665117]

Sadagopan S, Sharma-Walia N, Veettil MV, Raghu H, Sivakumar R, Bottero V, Chandran B. Kaposi's sarcoma-associated herpesvirus induces sustained NF-kappaB activation during de novo infection of primary human dermal microvascular endothelial cells that is essential for viral gene expression. J Virol 2007;81(8):3949–68. [PubMed: 17287275]

Salcedo R, Ponce ML, Young HA, Wasserman K, Ward JM, Kleinman HK, Oppenheim JJ, Murphy WJ. Human endothelial cells express CCR2 and respond to MCP-1: direct role of MCP-1 in angiogenesis and tumor progression. Blood 2000;96(1):34–40. [PubMed: 10891427]

Samaniego F, Pati S, Karp JE, Prakash O, Bose D. Human herpesvirus 8 K1-associated nuclear factor-kappa B-dependent promoter activity: role in Kaposi's sarcoma inflammation? J Natl Cancer Inst Monogr 2001;(28):15–23. [PubMed: 11158202]

Schwarz M, Murphy PM. Kaposi's sarcoma-associated herpesvirus G protein-coupled receptor constitutively activates NF-kappa B and induces proinflammatory cytokine and chemokine production via a C-terminal signaling determinant. J Immunol 2001;167(1):505–13. [PubMed: 11418689]

Sciacca FL, Sturzl M, Bussolino F, Sironi M, Brandstetter H, Zietz C, Zhou D, Matteucci C, Peri G, Sozzani S, et al. Expression of adhesion molecules, platelet-activating factor, and chemokines by Kaposi's sarcoma cells. J Immunol 1994;153(10):4816–25. [PubMed: 7963547]

Sharma-Walia N, Krishnan HH, Naranatt PP, Zeng L, Smith MS, Chandran B. ERK1/2 and MEK1/2 induced by Kaposi's sarcoma-associated herpesvirus (human herpesvirus 8) early during infection of target cells are essential for expression of viral genes and for establishment of infection. J Virol 2005;79(16):10308–29. [PubMed: 16051824]

Stamatovic SM, Keep RF, Mostarica-Stojkovic M, Andjelkovic AV. CCL2 regulates angiogenesis via activation of Ets-1 transcription factor. J Immunol 2006;177(4):2651–61. [PubMed: 16888027]

Tanimoto A, Murata Y, Wang KY, Tsutsui M, Kohno K, Sasaguri Y. Monocyte chemoattractant protein-1 expression is enhanced by granulocyte-macrophage colony-stimulating factor via Jak2-Stat5 signaling and inhibited by atorvastatin in human monocytic U937 cells. J Biol Chem 2008;283(8):4643–51. [PubMed: 18089573]

Uccini S, Scarpino S, Ballarini F, Soriani A, Chilosi M, Montesu MA, Masala MV, Cottoni F, Ruco L. In situ study of chemokine and chemokine-receptor expression in Kaposi sarcoma. Am J Dermatopathol 2003;25(5):377–83. [PubMed: 14501286]

Ueda A, Okuda K, Ohno S, Shirai A, Igarashi T, Matsunaga K, Fukushima J, Kawamoto S, Ishigatsubo Y, Okubo T. NF-kappa B and Sp1 regulate transcription of the human monocyte chemoattractant protein-1 gene. J Immunol 1994;153(5):2052–63. [PubMed: 8051410]

Vart RJ, Nikitenko LL, Lagos D, Trotter MW, Cannon M, Bourboulia D, Gratrix F, Takeuchi Y, Boshoff C. Kaposi's sarcoma-associated herpesvirus-encoded interleukin-6 and G-protein-coupled receptor regulate angiopoietin-2 expression in lymphatic endothelial cells. Cancer Res 2007;67(9):4042–51. [PubMed: 17483315]

Venetsanakos E, Mirza A, Fanton C, Romanov SR, Tlsty T, McMahon M. Induction of tubulogenesis in telomerase-immortalized human microvascular endothelial cells by glioblastoma cells. Exp Cell Res 2002;273(1):21–33. [PubMed: 11795943]

Wang L, Wakisaka N, Tomlinson CC, DeWire SM, Krall S, Pagano JS, Damania B. The Kaposi's sarcoma-associated herpesvirus (KSHV/HHV-8) K1 protein induces expression of angiogenic and invasion factors. Cancer Res 2004;64(8):2774–81. [PubMed: 15087393]

Wolter S, Doerrie A, Weber A, Schneider H, Hoffmann E, von der Ohe J, Bakiri L, Wagner EF, Resch K, Kracht M. c-Jun controls histone modifications, NF-kappaB recruitment, and RNA polymerase II function to activate the ccl2 gene. Mol Cell Biol 2008;28(13):4407–23. [PubMed: 18443042]

Yang TY, Chen SC, Leach MW, Manfra D, Homey B, Wiekowski M, Sullivan L, Jenh CH, Narula SK, Chensue SW, Lira SA. Transgenic expression of the chemokine receptor encoded by human herpesvirus 8 induces an angioproliferative disease resembling Kaposi's sarcoma. J Exp Med 2000;191(3):445–54. [PubMed: 10662790]

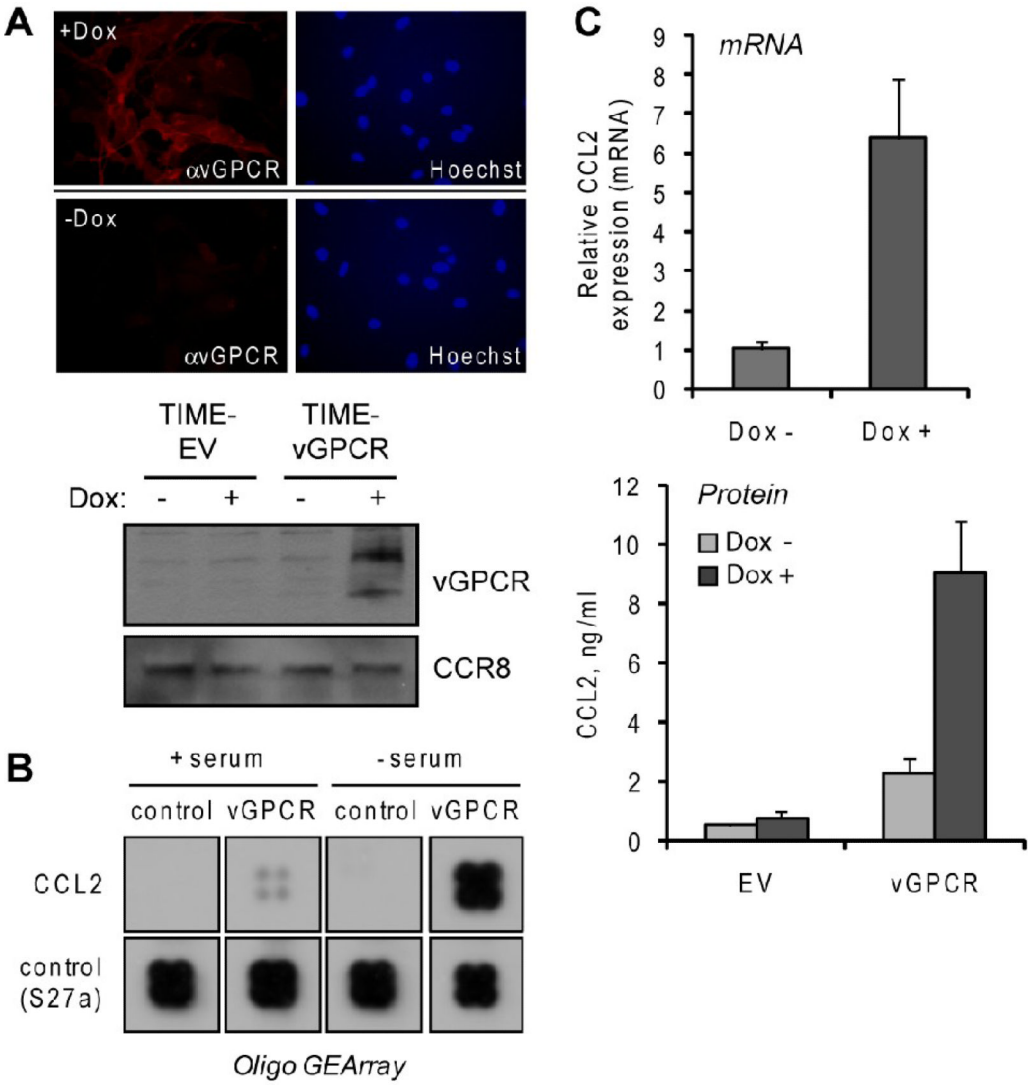

Figure 1.

Induction of CCL2 in vGPCR-transduced endothelial cells. **(A)** Testing of Tet-responsive element (TRE)-vGPCR transduced, rtTA transactivator-expressing TIME cells for Dox-inducible expression of vGPCR, visualized by using vGPCR rabbit antiserum (Chiou et al., 2002) in indirect immunofluorescence assay (top) and immunoblotting (bottom). EV, empty vector **(B)** Membrane hybridization analysis of CCL2 mRNA expression in TIME-vGPCR cells treated with Dox ($vGPCR^+$) or mock treated (control) for 24 h. Cells were either maintained in medium containing serum or serum-starved (to remove possible effects of serum-contained factors) for 24 h prior to addition of Dox. Extracted total RNA from these cultures were used to generate biotin-labeled cRNA probes for array hybridization (Materials and Methods). Sections of the array corresponding to CCL2 and "housekeeping" normalization control (RPSS27a, ribosomal protein) are shown. **(C)** Verification of array data for CCL2 induction by SYBR green-based qRT-PCR analysis of CCL2 mRNA levels (top) and ELISA quantitation of secreted protein (bottom) in Dox treated and untreated TIME-vGPCR cultures. qRT-PCR values were normalized to 18S RNA levels determined in parallel real-time PCR reactions; bars indicate deviations from the mean values of paired PCR reactions. For ELISA, duplicate cultures were analyzed and protein concentrations (in culture media) calculated from parallel standard-curve values.

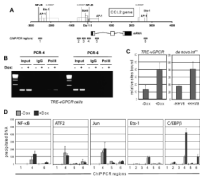

Figure 2.

Transcriptional analysis of vGPCR-mediated CCL2 induction. **(A)** Diagrammatic representation of the CCL2 gene, indicating regions and associated putative or demonstrated transcription factor binding sites implicated by previous studies in transcriptional regulation. Predicted C/EBP binding sites, identified by application of TFSEARCH (www.cbrc.jp/research/db/TFSEARCH.html) are shown in grey. The CCL2 mRNA structure is indicated, along with the map positions of the products of PCR primer pairs used for ChIP assays. **(B)** Ethidium bromide agarose gel analysis of PCR products derived from chromatin immunoprecipitation (ChIP) assays using antibodies to RNA polymerase II for precipitation of PolII-bound DNA. Two sets of primer pairs, one directed to proximal promoter sequences and the other to potential regulatory sequences 3' of the CCL2 gene, were used for PCR-mediated amplification of precipitated DNA. The former, specifically, was able to give rise to PCR products, which were increased in amplitude as a function of vGPCR expression (+Dox), indicative of receptor-mediated induction of CCL2 gene transcription. Normal IgG was used as a negative control to ensure specificity of DNA precipitation by PolII antibody. **(C)** Quantified ChIP data using primer pair 4 for qPCR analysis of PolII-associated and -precipitated DNA derived from Dox-treated or mock-treated TIME-vGPCR cells (left, TRE-vGPCR), confirming the data in panel B. Equivalent analysis of CCL2 promoter-associated PolII in response to HHV-8 *de novo* infection of TIME cells provided similar evidence of transcriptional induction of CCL2, 24 h post-inoculation (right, *de novo* inf^{n}). Error bars indicate deviation from mean values obtained from duplicate PCR reactions. **(D)** Analogous ChIP assays to investigate the potential relevance of a panel of transcription factors of possible relevance to vGPCR-mediated regulation of CCL2. Several PCR primer pairs (1-6) directed to different regions of the CCL2 locus were used for PCR amplification of precipitated DNA. Each was pre-validated to ensure ability to amplify “input” cellular DNA (data not shown). vGPCR-induced promoter-association of C/EBPβ, exclusively, was detected, specifically with regions amplified by PCR primer pairs 4 and 6 (right chart). Error bars indicate deviation from mean values obtained from duplicate PCR reactions.

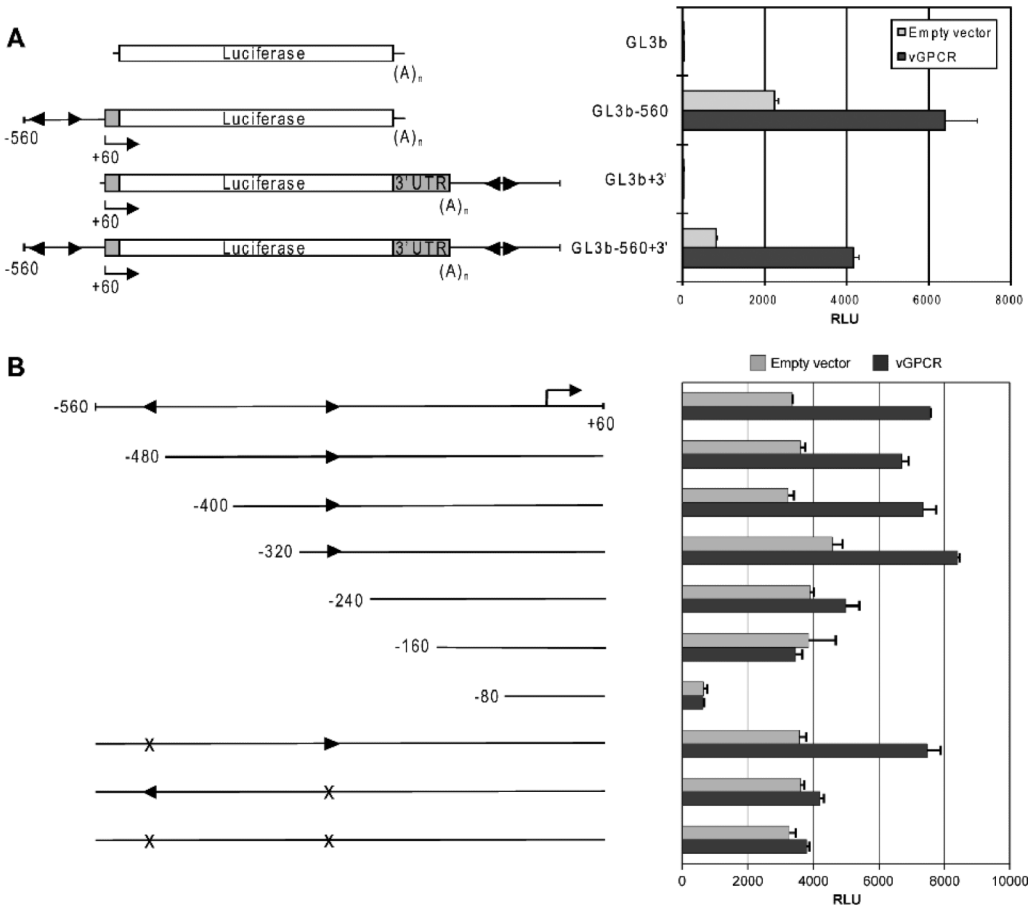

Figure 3.

Luciferase-based reporter assays to investigate possible contributions of 5' promoter and 3' regions to CCL2 induction by vGPCR. **(A)** Reporter constructions containing either or both of these regions were generated in pGL3basic (GL3b) transfected into HEK293T cells together with either vGPCR expression vector or empty vector control. The 5' region, corresponding to -560/+1, was activated by vGPCR, but the 3' sequences alone were unresponsive and did not contribute to vGPCR-induced luciferase expression when present with the 5' region. Error bars indicate standard deviations from mean values obtained from triplicate transfections. Arrowheads indicate putative C/EBPβ binding sites. **(B)** Analogous assays were undertaken using the -560/+1 reporter or deleted or C/EBP site-mutated versions thereof. The results obtained demonstrated the involvement of promoter-proximal sequences and specifically the -256/-263 C/EBP consensus site in vGPCR-mediated CCL2 induction. Mutation of the distal putative C/EBP-binding site did not affect CCL2 induction by vGPCR.

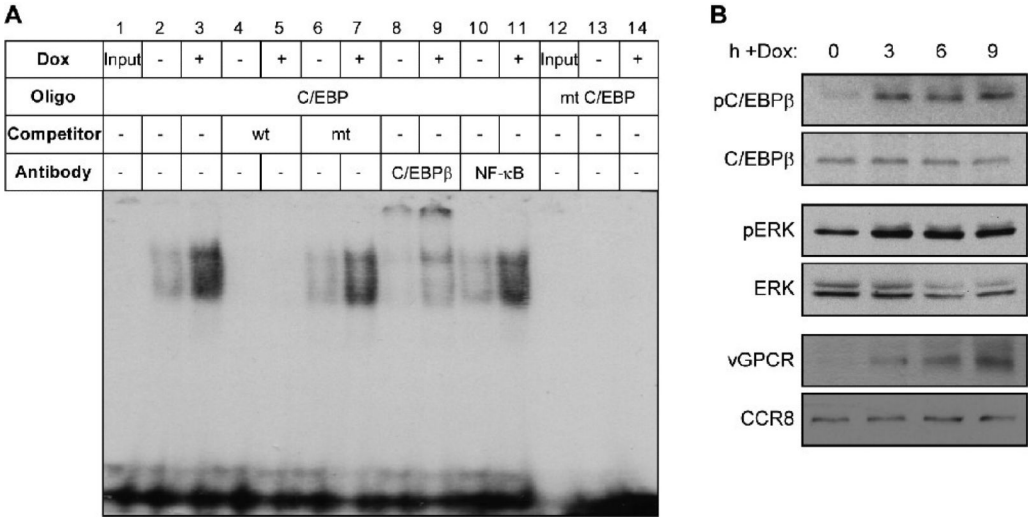

Figure 4.

C/EBPβ as a target of vGPCR activation. **(A)** EMSA for verification of C/EBPβ activation by vGPCR. A double-stranded, [^{32}P]-labeled probe containing a C/EBPβ binding core sequence was used to identify C/EBPβ activity in nuclear extracts of TIME-vGPCR cells, untreated or treated with Dox for 24 h. A probe mutated in the C/EBPβ binding sequence (mt C/EBP) was used as a control (lanes 12-14). Protein-DNA complexes were evident specifically on the wild-type probe, and these were induced by Dox treatment. The complexes could be supershifted with antibody specific for C/EBPβ, but not by antibody to NF-κB p65 (negative control), demonstrating the presence of C/EBPβ in the complexes. The complexes were also competed with excess unlabeled wild-type (wt) ds-oligonucleotide, but not by its mutated counterpart (mt). Input, probe loaded directly onto the gel without prior incubation with nuclear extract. **(B)** Immunobotting for detection of vGPCR-activated C/EBPβ. Antibody specific for Thr235-phosphorylated C/EBPβ was used to detect and determine relative levels of activated C/EBPβ in untreated TIME-vGPCR cells (time 0) and at various times (3 to 9 h) post-Dox induction of vGPCR expression. An appropriate antibody subsequently was applied to the stripped blot to detect total C/EBPβ, thereby providing a control for equal protein loading. Analogous analysis of induced phosphorylation (activation) of ERK (C/EBPβ kinase, targeting Thr235) also was undertaken (middle panels). Expression of vGPCR in response to Dox treatment of TIME-vGPCR cells was confirmed by western blotting; probing for chemokine receptor CCR8 provided a protein-load control (bottom two panels).

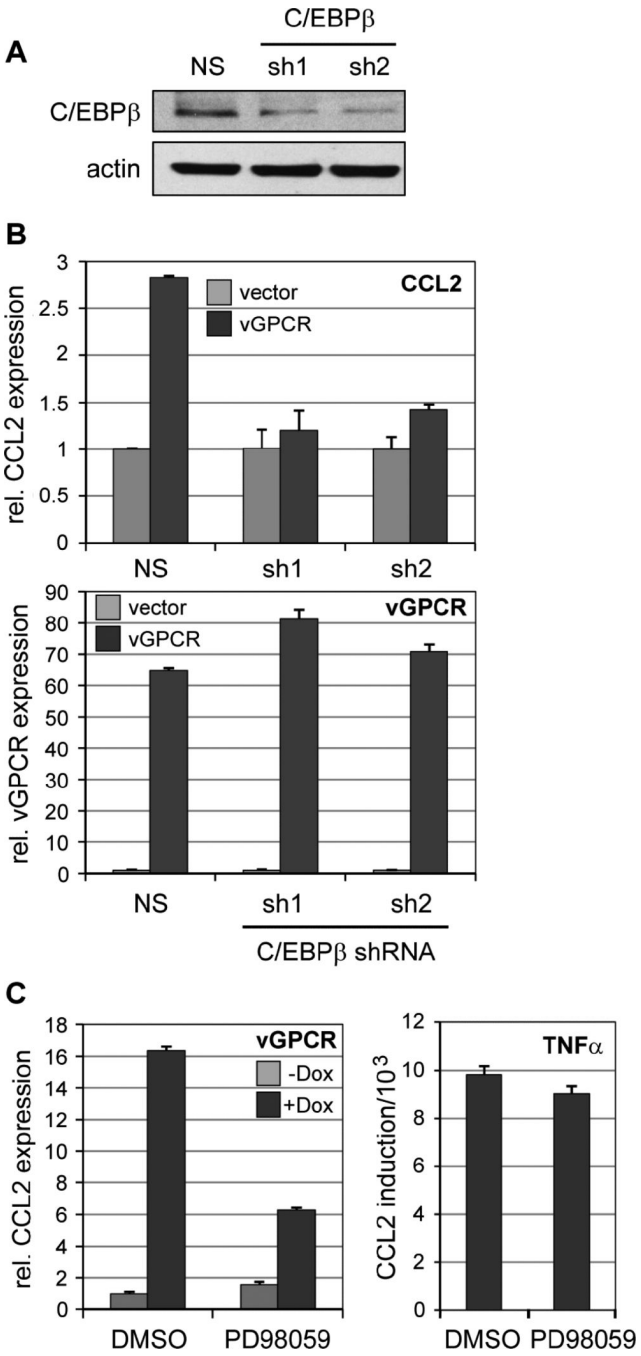

Figure 5.

C/EBPβ as a mediator of CCL2 induction by vGPCR. **(A)** Immunoblot-based analysis of C/EBPβ depletion in TIME-vGPCR cells transduced with either of two lentiviral vector-delivered shRNAs specific for C/EBPβ mRNA (sh1, sh2) as compared with control cells transduced with non-silencing (NS) shRNA. Actin antibody was used as a protein load control. **(B)** Dependency of vGPCR-induced CCL2 expression on C/EBPβ. NS or C/EBPβ shRNA-transduced TIME cells infected subsequently with vGPCR-encoding or empty lentivirus vectors were assessed by qRT-PCR analysis of extracted RNA for CCL2 mRNA expression. The data (top panel) revealed dependence of vGPCR-mediated induction of CCL2 on C/EBPβ expression, providing evidence of direct involvement of the transcription

factor in this response. Expression of vGPCR in receptor expression vector-transduced cells was verified by qRT-PCR (bottom panel). Error bars indicate deviation from mean values obtained from duplicate PCR reactions. **(C)** Involvement of MAPK signaling in vGPCR-mediated CCL2 induction. CCL2 mRNA expression was quantified by qRT-PCR, as before, in TIME-vGPCR cells mock treated or treated with Dox in the absence (DMSO) or presence of MEK (ERK kinase) inhibitor PD98059 (50 μM). The results (left) demonstrated substantial inhibition of CCL2 induction in the presence of PD98059. A parallel analysis of CCL2 induction by TNFα (10 ng/ml), which activates CCL2 via NF-κB signaling, showed no inhibition by the MEK inhibitor, thereby indicating the absence of non-specific effects mediated by drug treatment.

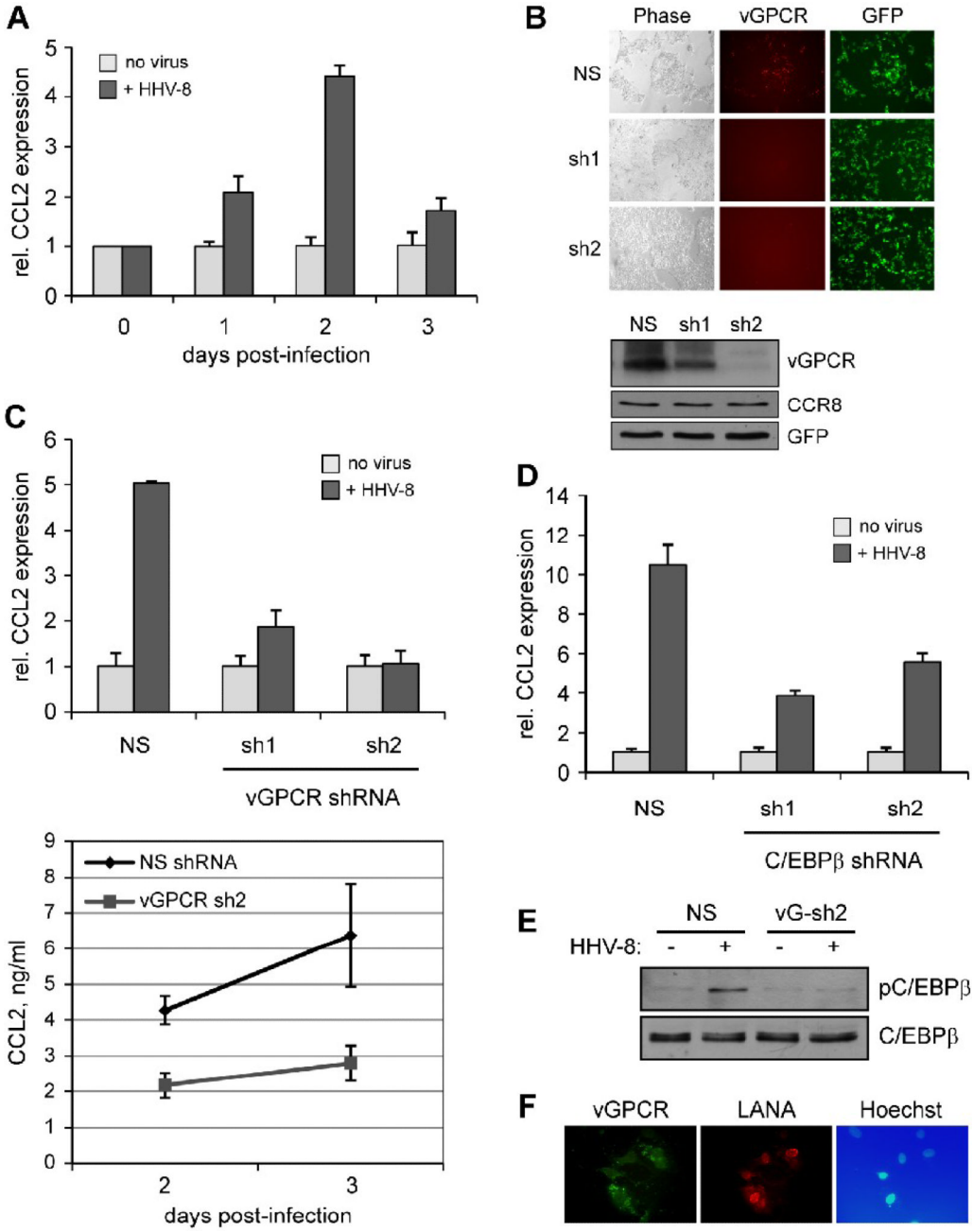

Figure 6.

Relevance of vGPCR and C/EBPβ to CCL2 induction in the context of HHV-8 infection. **(A)** Induction of CCL2 by HHV-8 infection. Cultures of TIME cells were infected with BCBL-1 cell-derived HHV-8 virus (see Materials and Methods). Infected and mock infected cultures were harvested at different times (0 to 3 days) after infection/mock infection, and extracted RNA analyzed by qRT-PCR to quantify relative mRNA levels (normalized to 18S RNA). **(B)** Testing of vGPCR-directed shRNAs for vGPCR depletion. First, two different vGPCR-specific shRNAs, cloned into GFP^+ lentiviral vectors, were tested by cotransfection with a vGPCR-RFP expression plasmid to determine their efficacies. Visualization of RFP by UV microscopy verified that each shRNA effectively depleted vGPCR-RFP expression, relative to non-silencing (NS) control. RFP fields for the vGPCR shRNAs (sh1, sh2) have

been deliberately overexposed to demonstrate very weak expression of vGPCR-RFP. vGPCR depletion by the receptor-directed lentiviral-cloned shRNAs was further tested using immunoblotting of transfected cell extracts; the results demonstrated significant depletion of vGPCR by both sh1 and sh2. **(C)** Stably-transduced TIME cultures expressing the vGPCR-specific shRNAs or NS control were infected or mock-infected with HHV-8 and cells harvested at 48 h for RNA extraction and qRT-PCR analysis of CCL2 mRNA and media collected at 48 h and 72 h for ELISA detection and quantitation of secreted CCL2 protein. In cells expressing the vGPCR shRNAs, the ability of HHV-8 *de novo* infection to induce CCL2 mRNA and protein expression was markedly reduced. **(D)** A similar, qRT-PCR-based experiment was undertaken in C/EBPβ-depleted TIME cells (Fig.5A). These cells, in contrast to NS-transduced TIME cells, were deficient in their ability to support CCL2 induction upon HHV-8 infection, confirming the importance of C/EBPβ for this response. **(E)** The role of vGPCR in C/EBPβ activation in HHV-8 infected cells was verified by comparison of C/EBPβ phosphorylation (on Thr235) in the absence and presence of shRNA-mediated vGPCR depletion. Western blotting of extracts from NS (control) and vGPCR shRNA-transduced cells revealed depleted phospho-C/EBPβ for the latter. **(F)** Detection of HHV-8 infection and vGPCR expression in *de novo* infected TIME cultures. TIME cultures, infected using identical conditions as before, were analyzed by IFA for detection of latency-associated nuclear antigen (LANA) and vGPCR. The results revealed high infection efficiency ($LANA^+$) and widespread expression of vGPCR in this population, consistent with functional data indicating the central role of vGPCR in CCL2 induction by *de novo* HHV-8 infection. In panels A, C and D, error bars indicate deviations of values from duplicate PCR reactions, or duplicate ELISA tests (panel C, bottom).